Two photon absorption in Mn²⁺-doped ZnSe quantum dots

Deepak More [a,1], Ch. Rajesh [a], Amit D. Lad [b], G. Ravindra Kumar [b], Shailaja Mahamuni [a,*]

[a] Department of Physics, University of Pune, Pune 411 007, India
[b] Tata Institute of Fundamental Research, Mumbai 400 005, India

ARTICLE INFO

ABSTRACT

The nonresonant third order nonlinear optical properties of three different sized Mn²⁺-doped ZnSe quantum dots (QDs) are investigated. The nonlinear absorption is measured at 532 nm using 35 picosecond laser pulses in an open-aperture Z-scan setup. Two photon absorption (2PA) cross-section in ZnSe QDs is found to be three orders of magnitude higher than its bulk value. These nanostructures show size dependent nonlinear absorption coefficients. It is found that the 2PA further enhances with decrease in size of the QD and is twice that of its undoped counterpart due to change in the local electric field.

© 2010 Elsevier B.V. All rights reserved.

1. Introduction

Confinement effects and high surface to volume ratio make quantum dots (QDs) promising electronic and optoelectronic materials. Their optical and electronic properties change drastically with size giving rise to large optical nonlinearities as well as fast response times. Recently, third order optical nonlinearity in various semiconductor QDs [1–10] has been studied in detail due to their potential applications in biological imaging, ultrafast optical switching, two photon microscopy, optical limiting, and optoelectronic devices [11–13]. ZnSe QDs are promising candidates for various optoelectronic devices in the blue region. Transition metal doped semiconductors show superior properties than undoped semiconductors QDs with greatly suppressed the host emission and improved thermal as well as chemical stability [14–18]. Such improved properties of doped semiconductors can be used in various practical applications like biomedical labelling and beads-based bar coding [14,15].

Multiphoton absorption (MPA) plays an important role in nonlinear absorption in various nanostructures. MPA has attracted great interest because (a) it can create excited states with photons of lower energy than the required excitation energy, and (b) the intensity dependence of MPA allows high degree of spatial selectivity in excitation. The nonresonant nonlinearities have faster response time as compared to resonant nonlinearities. 2PA is most commonly observed nonlinear phenomenon in QDs. 2PA is found to be enhanced in various semiconductor QDs [4–9] in comparison to their respective bulk counterparts.

There are various reports on Mn²⁺-doped ZnSe QDs focused mainly on synthetic procedure, luminescent mechanism, and time dependent measurements. Very few reports on nonlinear optical properties have been published [17]. In this communication, nonresonant third order nonlinear optical properties of undoped ZnSe as well as three different sized Mn²⁺-doped ZnSe QDs have been investigated and compared with nonlinear properties of bulk ZnSe. 2PA cross-section values in all QDs are found to be nearly three orders of magnitude higher than those in bulk ZnSe.

2. Experimental

The QDs were prepared by high temperature, organometallic synthesis reported by Norris et al. [18]. This procedure leads to highly crystalline, zinc-blende structure, and well passivated QDs. The undoped ZnSe QDs were synthesized by injecting the organometallic precursor containing diethylzinc and trioctylphosphine selenide (TOPSe) rapidly into the hot 1-hexadecylamine (HDA). The Mn²⁺-doped ZnSe QDs were synthesized in the identical experimental conditions, adding dimethylmanganese (MnMe₂) in the above mentioned organometallic precursor. In order to vary the size of Mn²⁺-doped ZnSe QDs the organometallic precursor was injected into the HDA at various temperatures. The particles are then isolated by standard procedure suggested by Hines and Sionnest [19] and finally a fine powder of undoped as well as Mn²⁺-doped ZnSe QDs is obtained.

The phase and size of undoped ZnSe and Mn²⁺-doped ZnSe QDs have been determined from X-ray diffraction (XRD). XRD studies were carried out using Bruker Axes D8 Advance powder X-ray dif-

* Corresponding author.
  E-mail addresses: grk@tifr.res.in (G.R. Kumar), shailajamahamuni@yahoo.co.in (S. Mahamuni).
  [1] Present address: K.J. Somaiya College of Sc. & Comm., Vidyavihar (E), Mumbai 400 077, India.
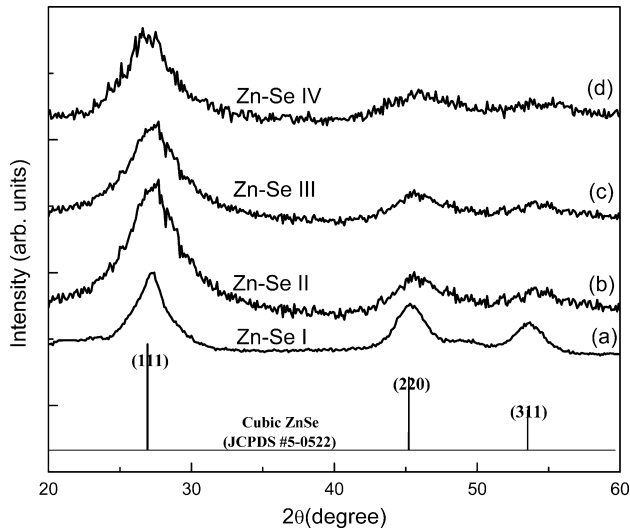
Fig. 1. XRD pattern of (a) undoped ZnSe (ZnSe-I) QDs of diameter 4.5 nm, as well as 7.5% Mn^{2+}-doped ZnSe QDs having diameters of (b) 3.6 nm (ZnSe-II), (c) 3.0 nm (ZnSe-III), and (d) 2.5 nm (ZnSe-IV).

fractrometer, using CuK_α ($\lambda = 1.5405$ Å) as an incident radiation. *TEM measurements are carried out using a Philips CM200 microscope operating at 200 kV.*

The amount of Zn, Mn, and Se in Mn^{2+}-doped ZnSe QDs is measured by inductively coupled plasma atomic emission spectroscopy (ICP-AES), carried out using a Spectro Arcos spectrometer.

The gap between the highest occupied molecular orbital (HOMO) and the lowest unoccupied molecular orbital (LUMO) of these QDs has been estimated from linear absorption spectroscopy. Linear absorption measurements have been performed using a Perkin Elmer Lamda 650, double beam spectrophotometer. The photoluminescence (PL) measurements have been carried out on Perkin Elmer LS55. Nonlinear absorption measurements are performed in a Z-scan set up using a hybrid mode-locked Nd:YAG laser emitting 532 nm, 35 picosecond pulses at a repetition rate of 10 Hz. The laser input beam is divided using beam splitter and one beam was used as reference beam. The other beam is focused with lens ($f = 27$ cm) onto the sample, with a focal spot of 23 µm diameter. The size of focal spot is obtained using knife edge method. The reference and transmitted beams are monitored by fast photodiodes. The peak intensities incident on the sample are maintained at 22 ± 2 GW/cm^2, to avoid damage of sample, quartz cuvettes are
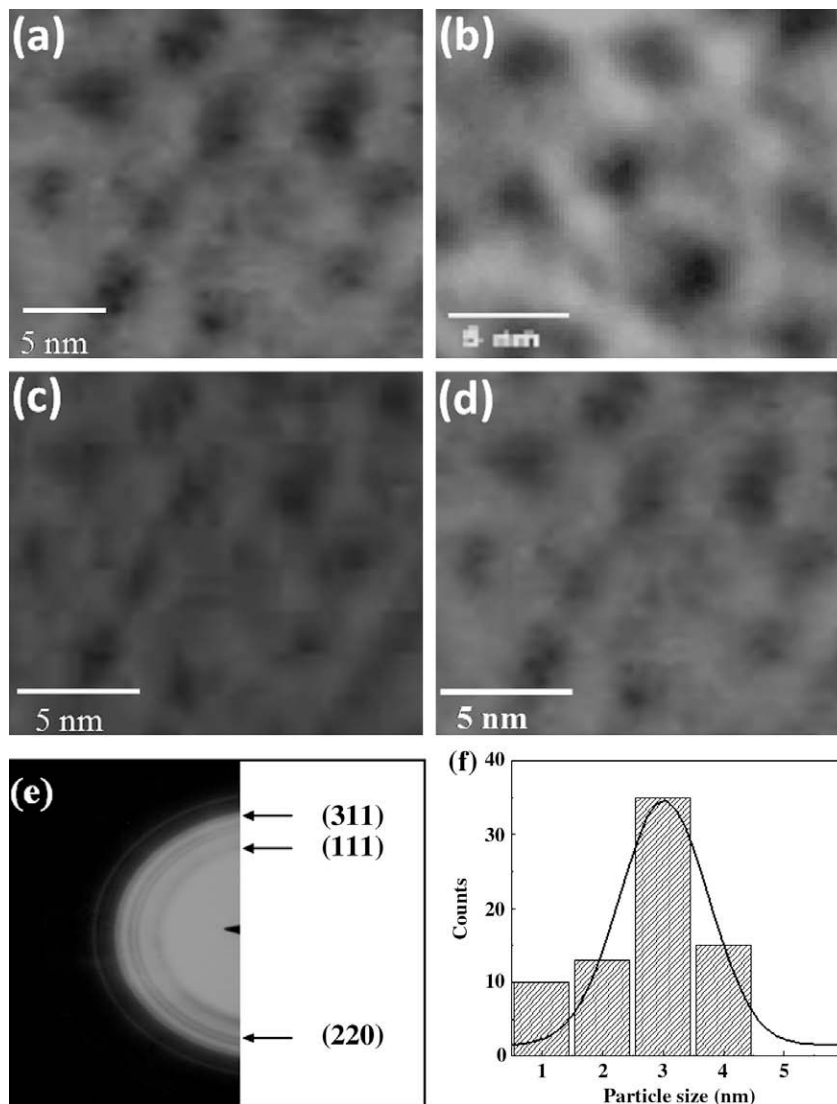

Fig. 2. TEM image of (a) undoped ZnSe QDs (ZnSe-I = 4.6 ± 0.4 nm), (b) ZnSe:Mn^{2+} quantum dots (ZnSe-II = 3.6 ± 0.3 nm), (c) ZnSe-III (3.1 ± 0.2 nm), and (d) ZnSe-IV (2.6 ± 0.4 nm), (e) Electron diffraction of ZnSe-IV and (f) Histogram indicating the size distribution of ZnSe-III.

Table 1

Size of the quantum dot is determined by XRD, TEM and by tight binding calculations. The percentage of Mn in solution as well as in the quantum dots has been tabulated.

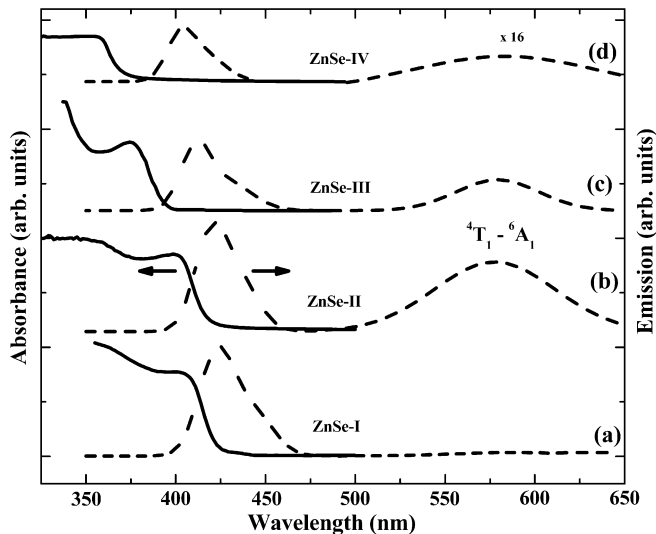|	Quantum dot size (nm)		Mn content (%)	
	XRD	TEM	Reaction solution	ZnSe QDs
ZnSe-I	4.5 ± 0.3	4.6 ± 0.4	0	0
ZnSe-II	3.5 ± 0.3	3.6 ± 0.3	7.5	0.76
ZnSe-III	3.0 ± 0.2	3.1 ± 0.2	7.5	0.11
ZnSe-IV	2.5 ± 0.2	2.6 ± 0.4	7.5	0.08

Fig. 3. Absorption spectra (solid lines) and PL (dashed lines) using an excitation wavelength of 350 nm of (a) undoped ZnSe QDs, (b), (c), and (d) are different sizes of Mn^{2+}-doped ZnSe QDs.

used for the measurements. QDs are dispersed in *n*-butanol and placed in a 1 mm of quartz cuvette. The transmittance is measured as a function of sample position (*Z*). *The reference and transmitted signals are fed to a Yokogawa DL 7200 digital oscilloscope, where they were recorded for all successive pulses.* Z-scan of distilled *n*-butanol is performed and it is found that there is no nonlinear absorption.

3. Results and discussion

XRD is used to determine the crystalline phase and average size of the QDs. Fig. 1 reveals cubic zinc-blende phase formation both in case of undoped as well as doped QDs. The average size of the QDs is determined using the Debye–Scherrer formula [20]. The average particle size of undoped ZnSe QDs is 4.5 ± 0.3 nm and we have varied the average size of Mn^{2+}-doped ZnSe QDs from 3.5 ± 0.3 to 2.5 ± 0.2 nm. TEM is employed to determine the size, shape, and crystal structure of the QDs (Fig. 2). The size of ZnSe-I, ZnSe-II, ZnSe-III, and ZnSe-IV QDs is found to be 4.6 ± 0.4, 3.6 ± 0.3, 3.1 ± 0.2 and 2.6 ± 0.4 nm. The electron diffraction pattern exhibits diffraction rings corresponding to (1 1 1), (2 2 0), and (3 1 1) lattice planes of cubic zinc-blende phase of ZnSe.

The Mn precursor concentration in the reaction solutions is kept constant i.e. 7.5%. ICP-AES measurements indicated a decrease in the Mn concentration in the QDs with decrease in size, but to a much lower level. The values are presented in Table 1. This observation is in conformity with the Mn related transition in PL spectra.

In case of undoped ZnSe QDs, the peak of linear optical absorption is at 410 nm, while it is blue shifted for Mn^{2+}-doped ZnSe QDs. The optical absorption feature for different sizes of 7.5% Mn^{2+}-

doped ZnSe QDs is found to be at 400, 376 and 355 nm (Fig. 3). The linear absorption spectrum clearly reveals the quantum size effects. Mn^{2+}-doped ZnSe QDs exhibit a very sharp excitonic feature indicating narrow size distribution.

Incorporation of Mn^{2+} in ZnSe QDs is confirmed by PL measurements (Fig. 2), as well as by electron paramagnetic resonance (EPR) [21]. PL spectra of Mn^{2+}-doped and undoped ZnSe QDs (Fig. 3) show strong blue emission around 425 nm. Blue emission is due to the band edge recombination. PL of Mn^{2+}-doped ZnSe QDs reveal an additional orange emission at 585 nm [21] due to Mn^{2+} ($^4T_1 \rightarrow {}^6A_1$) transition. Mn^{2+} *d–d* transition ($^4T_1 \rightarrow {}^6A_1$) is observed [22,23] at 585 nm in Mn^{2+}-doped ZnS nanoparticles as well.

Fig. 4 shows the open-aperture Z-scan data indicating a decrease of transmittance at position close to the focus, indicates nonlinear absorption. Fig. 4a shows that undoped ZnSe has absorption around 30% at focus. All Mn^{2+}-doped ZnSe QDs (Fig. 4b–d) show more absorption (35–47%) at the same intensity of incident beam at focus. For ZnSe-II (QD size 3.6 ± 0.3 nm) the absorption at focus is 33% and for ZnSe-IV (QD size 2.6 ± 0.4 nm) the absorption at focus is increased to 47%. This shows that as the size of sample decreases, the nonlinear absorption increases. 2PA coefficient β_2 can be calculated from following equations [24].

$$T(z) = \frac{1}{\sqrt{\pi}q_0} \int_{-\infty}^{+\infty} \ln[1 + q_0 \exp(-\tau^2)]d\tau \tag{1}$$

for $q_0 < 1$

$$T_{OA} = \sum_{m=0}^{\infty} (-1)^m \frac{q_0^m}{m+1})^{3/2} \tag{2}$$

where $q_0 = \beta_2 I_0 L_{eff}/(1 + z^2/z_0^2)$, I_0 is the on-axis instantaneous intensity of laser beam at the focus point, $L_{eff} = (1 - \exp(-\alpha_0 l))/\alpha_0$ is the effective length of the sample, α_0 is the linear absorption coefficient, and l is the length of the measured sample. The experimental data as shown in Fig. 4 is nearly symmetrical and has minimum at $Z = 0$. The 2PA coefficients can be obtained by fitting the open-aperture Z-scan traces by using Eq. (2). Fig. 4 solid line indicates that the theoretical curves match well with experimental data. 2PA coefficient per QD (β_{2QD}) has been evaluated and summarized in Table 2. This coefficient is related to the third order nonlinear susceptibility [$\chi^{(3)}$] by $\beta_2 = 3\pi \text{Im}[\chi^{(3)}]/\lambda n_0^2 c\varepsilon_0$, where n_0 is the linear refractive index, λ is wavelength of laser, c is speed of light in vacuum and ε_0 is dielectric constant of the material [25].

The energy of pump laser ($h\nu$) is 2.33 eV, which is significantly less than the band gaps (3.02–3.52 eV) of the QDs. The Mn^{2+}-doped ZnSe QDs have a strong absorption in the UV region (less than 300 nm) according to Fig. 4. It is reasonable that this nonlinear absorption effect for 532 nm is ascribed to the 2PA of Mn^{2+}-doped ZnSe QDs. The slope of graph of $\ln(1 - T)$ versus $\ln(I)$ is nearly equal to one which indicates that dip is due to two photon absorption (2PA) [9].

From the *2PA coefficients* (β_2), 2PA cross-section (σ_2) can be deduced as follows:

$$\sigma_2 = \frac{10^3 \beta_2 h\nu}{N_0 C} \tag{3}$$

where *C* is molar concentration. 2PA cross-section for ZnSe-I, ZnSe-II, ZnSe-III and ZnSe-IV are 1.0×10^{-46}, 1.8×10^{-46}, 1.95×10^{-46}, 2.33×10^{-46} cm^4 s/photon, respectively (Table 2). 2PA cross-section in ZnSe QDs is found to be three orders of magnitude higher than to its bulk value. Enhancement in 2PA cross-section is been observed in case of Mn^{2+}-doped ZnSe QDs compared to undoped ZnSe QDs. The intrinsic 2PA coefficient of QDs (γ_{QD}) can be deduced as $\gamma_{QD} = \beta_{2solution} n_{0solution}^2/(n_{0QD}^2 f_v |f|^4)$, where f_v is volume fraction of QDs in the solution, and f is local field correction depending upon the dielectric constant of material and solution. The enhancement
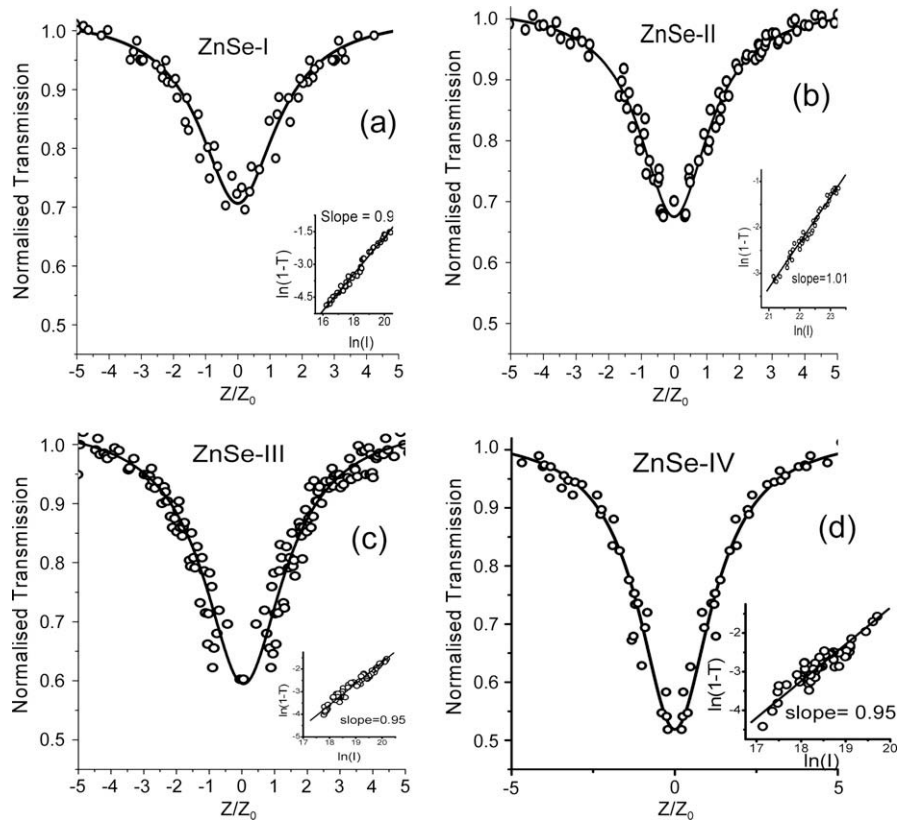
Fig. 4. Open aperture Z scan curves for ZnSe and Mn^{2+} doped ZnSe QDs at input intensity of 22 GW/cm^2. Solid line is theoretical fit to experimental data (symbols). The insets show the scaling for 2PA. (a) 4.5 nm (Undoped ZnSe-I), (b) 3.0 nm (ZnSe-II), and (c) 3.6 nm (ZnSe-III) (d) 2.5 nm (ZnSe-IV).

Table 2
Linear absorption, diameter, 2PA coefficient, intrinsic 2PA coefficient per QD, and 2PA cross-section of QDs dispersed in *n*-butanol.

	Linear absorption (eV)	Diameter estimated by XRD (nm)	2PA coefficient per QD β_{2QD} (cm/GW)	Intrinsic 2PA coefficient γ_{QD} (cm/GW)	2PA cross-section σ_2 (cm^4 s/ photon)
ZnSe-I	3.04	4.5	6.4×10^{-13}	9.27	1.0×10^{-46}
ZnSe-II	3.12	3.6	7.5×10^{-13}	10.87	1.8×10^{-46}
ZnSe-III	3.32	3.0	8.1×10^{-13}	11.73	2×10^{-46}
ZnSe-IV	3.52	2.5	9.8×10^{-13}	14.20	2.3×10^{-46}
Bulk ZnSe[a]	2.67			–	6.9×10^{-49}

[a] Ref. [26].

in intrinsic 2PA coefficient (Table 2) is observed with reduction in size of the QD due to quantum confinement effects and modified local field effects [26].

It is shown that by increasing the thickness of ZnSe layer on dopants (Mn^{2+}), the quantum yield of QDs can be improved. But as this thickness increases, the value of 2PA coefficient saturates and hence size of QD matters [17]. Since the light emitters are dopant Mn^{2+} ions, it helps to decrease the local field correction factor with decrease in the size of QD. This results into increase in the intrinsic 2PA coefficient values. In certain applications such as optical limiting devices, one might demand high nonlinear coefficient for certain wavelength regions.

4. Conclusions

We have investigated nonlinear optical properties of high quality Mn-doped ZnSe QDs and found that 2PA is dominant mechanism in Mn^{2+}-doped ZnSe QDs at incident excitation photon energy of 2.33 eV. Further 2PA cross-section is found to be en-

hanced with the decrease in the diameter of QDs. The increase in nonlinearity with decrease in the quantum dot diameter is attributed to quantum size effects and change in the local field. Such dot-size dependent nonlinearity can be very useful in ultrafast switching and optical limiting devices at higher intensities.

References

[1] J. He, W. Ji, G.H. Ma, S.H. Tang, H.I. Elim, W.X. Sun, Z.H. Zhang, W.S. Chin, J. Appl. Phys. 95 (2004) 6381.
[2] L. Padilha, J. Fu, D.J. Hagan, E.W.V. Stryland, Opt. Exp. 13 (2005) 6460.
[3] Y.C. Ker, J.H. Lin, W.F. Hsieh, Jpn. J. Appl. Phys. 42 (2003) 1258.

[4] V.V. Nikesh, A. Dharmadhikari, H. Ono, S. Nozaki, G.R. Kumar, S. Mahamuni, Appl. Phys. Lett. 84 (2004) 4602.
[5] J. He, J. Mi, H. Li, W. Ji, J. Phys. Chem. B 109 (2005) 19184.
[6] I. Gerdova, A. Haache, Opt. Commun. 26 (2005) 205.
[7] X. Wang, Y. Du, S. Ding, Q. Wang, G. Xiang, M. Xie, X. Chen, D. Peng, J. Phys. Chem. B 110 (2006) 1566.
[8] Y. Qu, W. Ji, Y. Zheng, J.Y. Ying, Appl. Phys. Lett. 90 (2007) 133112.
[9] A.D. Lad, P.P. Kiran, D. More, G.R. Kumar, S. Mahamuni, Appl. Phys. Lett. 92 (2008) 043126.
[10] A.D. Lad, P.P. Kiran, G.R. Kumar, S. Mahamuni, Appl. Phys. Lett. 90 (2007) 133113.
[11] G. Konstantatos, I. Howard, A. Fischer, S. Hoofland, J. Clifford, E. Klem, L. Levina, E.H. Sargent, Nature 442 (2006) 180.
[12] B. Deberret, P. Skorides, D.J. Norris, V. Noireaux, A.H. Brivanlou, A. Libchaber, Science 298 (2002) 1759.
[13] X. Michalet, F.F. Pinaud, L.A. Bentolila, J.M. Tsay, S. Doose, J.J. Li, G. Sunderesan, A.M. Wu, S.S. Gambhir, S. Weiss, Science 307 (2005) 538.
[14] N. Pradhan, D. Goorskey, J. Thessing, X. Peng, J. Am. Chem. Soc. 127 (2005) 17586.

[15] N. Pradhan, D.M. Battaglia, Y. Liu, X. Peng, Nano Lett. 7 (2007) 312.
[16] M. Han, X. Gao, J.Z. Su, S. Nie, Nat. Biotechnol. 19 (2001) 631.
[17] C. Gan, M. Xiao, D. Battaglia, N. Pradhan, X. Peng, Appl. Phys. Lett. 91 (2007) 201103.
[18] D.J. Norris, N. Yao, F.T. Charnock, T.A. Kennedy, Nano Lett. 1 (2001) 3.
[19] M.A. Hines, P.G. Sionnest, J. Phys. Chem. B 102 (1998) 3655.
[20] B.D. Cullity, Elements of X-ray Diffraction, Addison-Wesley, New York, 1977.
[21] A.D. Lad, C. Rajesh, M. Khan, N. Ali, I.K. Gopalakrishnan, S.K. Kulshrestha, S. Mahamuni, J. Appl. Phys. 101 (2007) 103906.
[22] R.N. Bhargava, J. Lumin. 70 (1996) 85.
[23] H.S. Bhatti, R. Sharma, N.K. Verma, N. Kumar, S.R. Vadera, K. Manzoor, J. Phys. D: Appl. Phys. 39 (2006) 1754.
[24] M.S. Bahae, A.A. Said, T.H. Wei, D.J. Hagan, E.W.V. Stryland, IEEE J. Quantum Electron. 26 (1990) 760.
[25] Handbook of Nonlinear Optics, second ed., Richard L. Sudherland-Marcel Dekker Inc., New York.
[26] H.S. Brandi, C.B. Araujo, J. Phys. C: Solid State Phys. 16 (1983) 5929.